Journal of CO2 Utilization 83 (2024) 102775

Contents lists available at ScienceDirect

Journal of CO2 Utilization

journal homepage: www.elsevier.com/locate/jcou

Experimental assessment of reverse water gas shift integrated with chemical looping for low-carbon fuels

Syed Zaheer Abbas [a,b], Christopher de Leeuwe [a], Alvaro Amieiro [c], Stephen Poulston [c], Vincenzo Spallina [a,*]

[a] Department of Chemical Engineering, School of Engineering, University of Manchester, Booth St E, Manchester, Manchester M13 9PL, United Kingdom
[b] Department of Chemical Engineering, University of Southampton, University Road, Southampton SO17 1BJ, United Kingdom
[c] Johnson Matthey Technology Centre, Reading RG4 9NH, United Kingdom

ARTICLE INFO

Keywords:
Chemical looping
CCU
Reverse water gas shift
Syngas production
Net zero emissions

ABSTRACT

Chemical looping integrated with reverse water gas (CL-RWGS) shift is presented in this study using Cu-based oxygen carrier (OC) supported on Al_2O_3 has been used to convert the CO_2 and H_2 mixture stream into a syngas stream with a tailored H_2 to CO ratio and relevant conditions. The results demonstrated consistent breakthrough curves during redox cycles, confirming the chemical stability of the material. In 10 consecutive cycles at 600 °C and 1 bar, bed temperatures increased by 184 °C and 132 °C across the bed during oxidation and reduction stages respectively. The cooling effects during RWGS showed a decline in solid temperatures demonstrating the effectiveness of the heat removal strategy while attaining a CO_2-to-CO conversion close >48%. The outlet gas maintains a H_2/CO ratio above 2, confirming the material's dual role as OC and catalyst. During complete CL-RWGS cycles, varying temperature from 500 °C to 600 °C at a constant H_2/CO_2 molar ratio (1.3) and pressure (1 bar) reduces the H_2/CO molar ratio from 3.14 to 2.35, respectively with a remarkable continuous CO_2-to-CO conversion > 40%. The decrease in H_2/CO molar ratio with the increase in temperature is consistent with the expected results of equilibrium limited conditions. Additionally, in CL-RWGS cycles, pressure insignificantly affects product molar composition. The study showed the capability of Cu material in converting CO_2 into syngas through the CL-RWGS technique.

1. Introduction

In the recent past, the awareness of global warming has led policy-makers to modify the energy and environmental plan to meet the ambitious target of net zero by 2050. This includes the reduction of CO_2 emissions by 50% to its level in 2005 [1]. Industry roughly produces 15 $GtCO_2$ of direct CO_2 annually, constituting approximately 40% of all CO_2 emissions from energy-related sources. Energy-intensive industries like iron and steel, cement, refineries and other petrochemical industries are the major CO_2 production sources and annually contribute around 10 $GtCO_2$ to the atmosphere [2]. Carbon capture and storage (CCS) is among the key solutions to reduce CO_2 from the atmosphere [3]. Apart from permanent CO_2 storage carbon capture and utilization (CCU) is among solutions to produce values added chemicals like liquid fuels or methanol [4]. On the other hand, liquid fuels annual consumption is around 3 billion tons which is equivalent to approximately 9Gt CO_2 to be used for production, an approximately 30% reduction of total CO_2 emission [5,6]. In combination with green hydrogen produced by renewable energy, CCU could unlock carbon neutral fuels.

The reverse water gas shift (RWGS) process is one of the widely known techniques for the conversion of CO_2 to CO which can later be used for the production of valued added chemicals like liquid fuels through a well-known synthesis gas (CO and H_2) conversion techniques, such as Fischer-Tropsch Synthesis (FTS) [5].

As an endothermic reaction, the RWGS requires high temperature (> 800°C) heat which is the main energy penalty and would generate additional CO_2 emissions if combined with conventional thermochemical technologies. Therefore, several process and reactor concepts have been proposed lately which could make more efficient and environmentally friendly syngas generation from CO_2. Externally heated RWGS concepts have already found a route to commercialisation with major companies already developing the technology (Johnson Matthey [7], Topsoe [8] among others). Other developments include the intensification of the process to achieve higher efficiency. This is the case of

* Corresponding author.
E-mail address: vincenzo.spallina@manchester.ac.uk (V. Spallina).

https://doi.org/10.1016/j.jcou.2024.102775
Received 26 February 2024; Received in revised form 3 April 2024; Accepted 19 April 2024
Available online 24 April 2024

RWGS membrane reactor using zeolite membranes for the selective separation of H_2O which would shift the CO_2-to-CO conversion further the equilibrium [9], fully electrified reactors to reduce the reactor size and footprint [10] and plasma-assisted process to activate the catalyst and enhance locally the CO_2 conversion [11] to CO or even further to methanol [12,13]. A more comprehensive review of the process from a process system engineering perspective has been published by Gonalez-Castaño et al. [14].

The application of chemical looping to RWGS has been studied primarily in terms of CO_2-to-CO reduction [15–17]. Makiura et al. [18] tested Co–In_2O_3 showing a high CO_2 splitting rate in the mid-temperature range (723–823 K). Daza et al. [19–21] studied LaSrCo-based perovskites to alternate H_2 oxidation and CO_2 reduction as material to decouple RWGS, while Lee et al. [22] developed a core-shell catalyst based on $La_{0.75}Sr_{0.25}FeO_3$-encapsulated Co_3O_4-NiO to enhance the stability of the material while Orsini et al. [23] succesfully tested the activity of $Sr_2FeMo_{0.6}Ni_{0.4}O_{6-\delta}$ double perovskite. All these materials suffer from a low oxygen transport capacity which depends on the oxygen vacancies created in the perovskite lattice. To increase it, Bulfin et al. [24] have operated a 1 m counter-current unit at 800°C using $CeO_{2-\delta}$ which could increase the conversion up to 88% (compared to the thermodynamic limit of 58%). Despite the growing effort to develop more stable and active materials for direct CO_2-to-CO conversion, the application of direct chemical looping for CO production has not yet been demonstrated; in addition, the effect of gas velocity, temperature and pressure dependence on the performance and actual process footprint is unknown and requires further development and effort from the scientific community and industry. An alternative approach to combine chemical looping and RWGS consists of using the heat generated during the combination of reduction-oxidation of the oxygen carrier and then allowing the H_2 and CO_2 conversion to CO-rich syngas while cooling the bed. This approach has been widely demonstrated for the chemical looping reforming with packed bed reactors [22,25,26] and some initial evidence of the process where reported by De Leeuwe et al. [22]. In this case, the RWGS is kept as a catalytic reaction and the CO_2-to-H_2 conversion exclusively depends on the reactor operating conditions and material that would catalyse the reaction, typically Cu, Ce, Ni, Fe-based and multicomponent metal oxides [5,27–31]. Moreover, this concept enables the use of any sort of offgas at the reduction (blast furnace offgas, liquid waste stream, flare gases, PSA offgas, etc.) without interfering with the RWGS reaction.

In this work, CL-RWGS for the intensified conversion of CO_2 and H_2 to syngas has been carried out in packed-bed reactors. As illustrated in Fig. 1, the packed-bed reactors are dynamically operated to carry out the three main reaction stages: Cu-oxidation with air or O_2-rich stream, CuO reduction using low-grade fuel and the RWGS by feeding a mixture of H_2 and CO_2. The main chemical reactions that take place in the CL-RWGS process are tabulated in Table 1. Such a process could rely on the existing knowledge generated over the past 20 years on oxygen carrier materials thus facilitating the scale-up and implementation while removing a critical bottleneck.

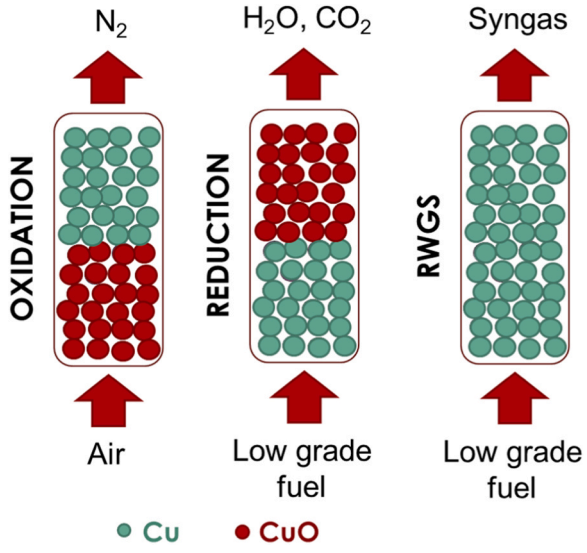

Fig. 1. Schematic diagram of the CL-RWGS process for the CO_2 conversion to syngas proposed in this study.

This study presents a founding demonstration of a pseudo-continuous CL-RWGS process in a lab-scale packed bed reactor, operating under high-pressure and flowrate conditions, marking the first of its kind in the literature. Moreover, it verifies several previously formulated hypotheses by testing gas-solid looping beyond atmospheric pressure and flowrate, while also investigating process operation using existing materials, thereby laying the groundwork for further scale-up and demonstration. Furthermore, no prior study has shown the thermal integration of RWGS with chemical looping, underscoring the importance of our comprehensive evaluation at temperatures and bed capacities relevant to lab-scale setups, as well as under high pressure, to guarantee the production of syngas of adequate quality for downstream FTS. By focusing on reactor engineering principles and offering a thorough examination of the process's thermal dynamics, these discoveries are crucial for advancing the technology to larger scales while opening up new possibilities for RWGS applications. The novelty and timely innovation of this work relies on demonstrating the feasibility of the CL-RWGS under relevant conditions over the three key stages. The experimental campaign has been focused on high temperature, high pressure, high feed flow rate and composition ($H_2/CO_2 = 0.2 – 2.0$). In addition, the process has been tested for 10 continuous cycles of oxidation/reduction and RWGS with controlled heat losses. This work is therefore informative for the industry to identify new transition technology with efficient thermal management, inherent CO_2 utilisation, offgas recovery and syngas generation.

2. Material and methodology

2.1. Lab-scale experimental setup

The experimental campaign of CL-RWGS process has been carried out the at University of Manchester (Fig. 2a–c). The setup consists of fully integrated miniplant with dry gas feeding (H_2, N_2, He, CH_4, CO, CO_2, and air), a packed-bed reactor, manufactured by Array industries B. V, having 1050 mm length and 35 mm inside diameter Fig. 2(b) which is heated by Carbolite® furnace and equipped with a K-type multipoint thermocouple (10 measuring points), manufactured by Endress+Hauser Ltd. The gas composition is measured using CO analyser (Siemens) and a Hiden QGA mass spectrometer (MS). The P&ID of the experimental setup has been shown in Fig. 3. Further details of the setup are reported in Argyris et al. [32].

2.2. Oxygen carrier material

250 g of Cu-based OC (Fig. 4) supplied by Johnson Matthey was crushed to get an average particle size of 1.5–2 mm using Pulverized Ball

Table 1
Chemical reactions considered in the CL-RWGS process.

Process	Reaction		
Oxidation	$2\,Cu_{(s)} + O_{2(g)} \rightarrow 2\,CuO_{(s)}$	$\Delta H_{298\,K} = -310.4\ kJ\ mol^{-1}$	(R1)
Reduction (with H_2)	$CuO_{(s)} + H_{2(g)} \rightarrow Cu_{(s)} + H_2O_{(g)}$	$\Delta H_{298\,K} = -86.6\ kJ\ mol^{-1}$	(R2)
Reverse Water gas shift (RWGS)	$H_{2(g)} + CO_{2(g)} \rightarrow CO_{(g)} + H_2O_{(g)}$	$\Delta H_{298\,K} = 41.2\ kJ\ mol^{-1}$	(R3)

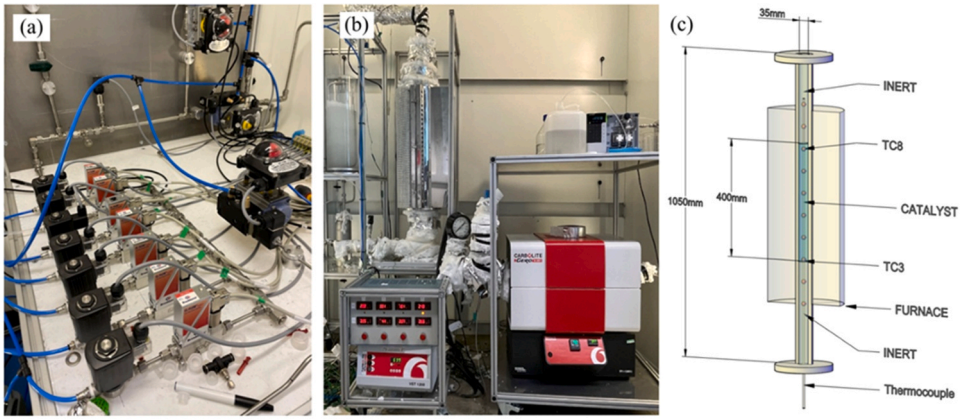

Fig. 2. The packed bed reactor assembly at the University of Manchester having (a) FC-1 consists of gas feeding system and mass flow controllers; (b) FC-2 where packed bed reactor enclosed in a furnace has been and (c) schematic diagram of the packed-bed reactor unit.

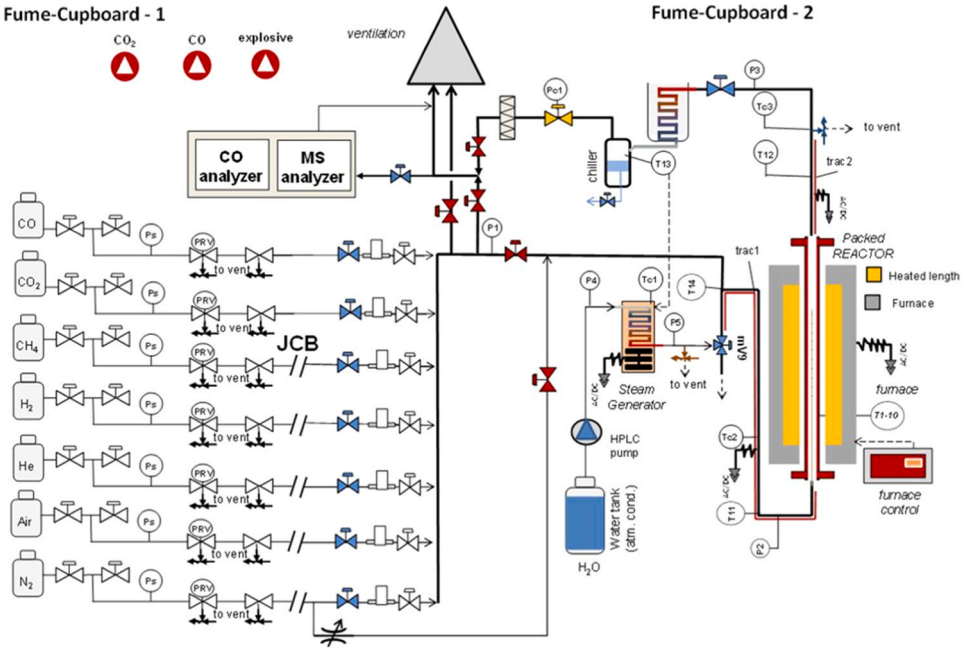

Fig. 3. P&ID of the experimental setup located in University of Manchester.

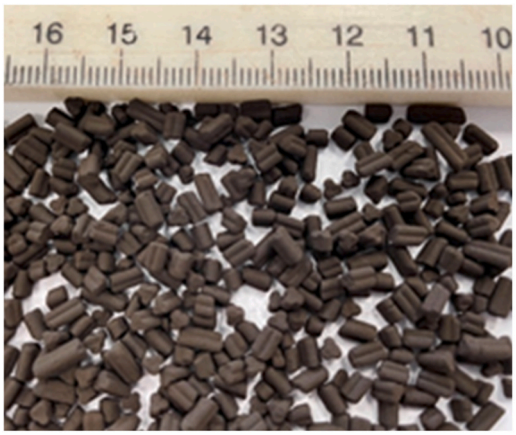

Fig. 4. Image of the C-based oxygen carrier (OC) used in this experimental study.

mill has been packed inside the reactor, 400 mm bed length, with the top and bottom part of the reactor fully packed with inert material (Al_2O_3). Further details regarding the utilized material can be found in the literature [33,34]. Inert material at the top and bottom of the reactor is used to make sure that OC is firmly packed inside the reactor throughout the CL-RWGS experimental campaign. Throughout the inlet and outlet of the reactor, heating lines are used to make sure that no condensation takes place at any stage during the process. More details about the material used in this study are reported in other studies [25,35,36] in which pre and post-testing characterisation, redox kinetics and long-term stability are extensively discussed for the relevant conditions used in this study. Since the gas-solid reactions and particle behaviour do not differ from previous works, it was not addressed in this manuscript.

2.3. Design of the experiments

During the first stage, Cu oxidation stage, diluted air feed (10% O_2 in feed) is used to oxidize the Cu-based particles through the Cu-oxidation reaction (R1) at high pressure (1 – 5 bar) and moderate temperature

(500 – 600 °C). This results in an O_2-depleted stream leaving the reactor and a highly exothermic oxidation reaction ($\Delta H_{298\,K} = -310.4$ kJ mol^{-1}) causes a considerable rise in reactor temperature. Once Cu is completely oxidized, in the second reaction stage, the reactor is fed with a fuel mixture to reduce the solid bed at the same operating temperature and pressure as that of the oxidation stage. The exothermic nature of CuO reduction with H_2 (R2, $\Delta H_{298\,K} = -86.6$ kJ mol^{-1}) provides the necessary heat for the final stage of the CL-RWGS process (RWGS stage). In the final stage, RWGS stage, H_2 reacts with CO_2 (R3) and produces H_2/CO gas (syngas). The experimental campaign and operating conditions are tabulated in Table 2. In between the reaction stages, the reactor was purged with N_2 to remove the unwanted gases from the reactor in order to avoid any undesired reaction to take place in the reactor. Purging with N_2 also prepared the reactor for the next reaction stage.

3. Results and discussion

3.1. Material activation

Prior to the CL-RWGS comprehensive testing campaign, 10 consecutive cycles of oxidation-reduction (redox) were conducted to activate the material before further testing for the CL-RWGS process. The activation was carried out in the same reactor used for subsequent testing. After 10 cycles, steady cycling behaviour was seen in the outlet gas composition, with cycles 8, 9 and 10 being indistinguishable from each other. This demonstrates that the material has been activated and is prepared for subsequent testing. Fig. 5 (a) shows the O_2 breakthrough curve over 10 consecutive cycles of oxidation at 600 °C, 1 bar and 10% O_2 in feed. It can be seen that the O_2 breakthrough curves are quite reproducible (approximately 6 minutes), hence showing that the material reached a stable behaviour. Cu oxidation causes a rise of 184 °C in temperature across the packed bed reactor as can be seen in Fig. 6 (a). Similarly, the Cu-based OC is tested for reduction cycles. Fig. 5 (b) shows the H_2 curves during the first cycle of reduction at 600 °C, 1 bar and 20% H_2 in feed. The reduction of CuO using H_2 as a reducing gas is also an exothermic reaction ($\Delta H_{298\,K} = -86.6$ kJ mol^{-1}) and it causes a rise of 132 °C across the bed as shown in Fig. 6 (b).

Table 2
The lab-scale conditions used during the CL-RWGS process.

Process conditions	Oxidation stage	Reduction stage	Reverse water gas shift stage
Temperature [°C]	600	600	650 – 900
Pressure [bar]	1 – 5	1 – 5	1 – 8
H_2/CO_2 molar ratio	——	——	2 – 0.2
Feed gas composition (vol %)	10% O_2 in Air	20% H_2, 10% He and 70% N_2	1) 25% H_2, 12.5% CO_2, 12.5% He and 50% N_2 2) 33.3% H_2, 25% CO_2, 8.3% He and 33.3% N_2 3) 14.3% H_2, 14.3% CO_2, 14.3% He and 57% N_2 4) 18.2% H_2, 36.4% CO_2, 9% He and 36.4% N_2 5) 11% H_2, 33.3% CO_2, 11% He and 44.4% N_2 6) 10% H_2, 40% CO_2, 10% He and 40% N_2 7) 9.1% H_2, 45.5% CO_2, 9.1% He and 36.4% N_2
Total volumetric flow (NLPM)	10	10	10 – 16

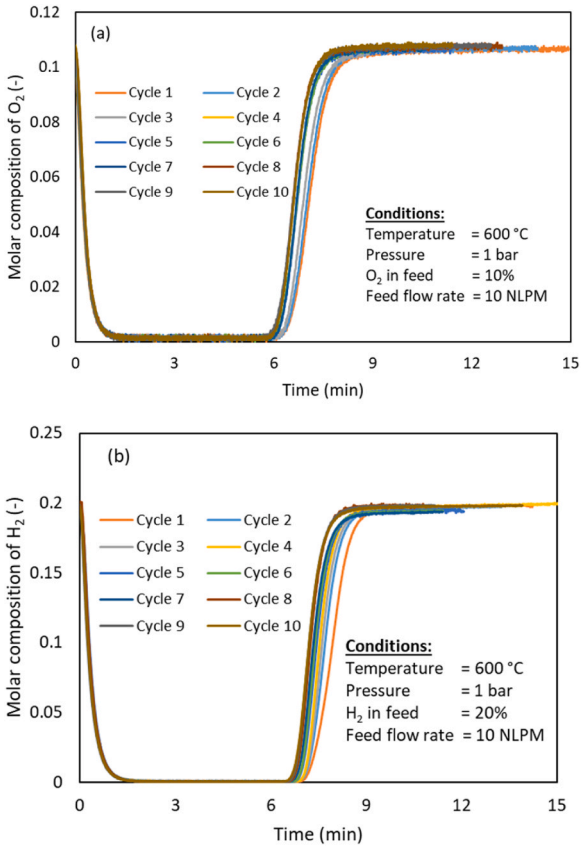

Fig. 5. (a) Evolution of O_2 curves during the Cu oxidation and (b) CuO reduction over 10 cycles.

For both oxidation and reduction, the cycle time to breakthrough is identical since stoichiometric feed gases (O_2/H_2 mol ratio = 0.5) are fed, thus the system behaves as a stochiometric combustor.

The breakthrough time obtained during the oxidation cycles helped to set the cycle time for oxidation during the complete cycle of CL-RWGS process.

In Abbas et al. [40], the morphology and the degradation of the Cu-based material via SEM technique were observed and the material did not show any degradation after testing for over 100 hrs of operation at severe temperature (~950 °C) and pressure (~8 bar) conditions.

3.2. Reverse water gas shift stage

As indicated in Table 2, Cu-based OC is tested for RWGS process under various conditions. Fig. 7(a – b) illustrates the product gas composition (on dry basis) and temperature across the reactor during the RWGS at 900 °C, 1.0 bar and a feed gas composition of H_2/CO_2 molar ratio of 1.0. The product molar composition stayed steady throughout the RWGS process and shows a H_2/CO molar ratio of 1.4. The results in Fig. 7(b) show also a solid temperature drop across the reactor length which indicates that the reaction is endothermic (RWGS $\Delta H_{298\,K} = +41.2$ kJ mol^{-1}).

The H_2/CO value showed that operating conditions (temperature, pressure and H_2/CO_2 molar ratios) need to be varied to get the H_2/CO ratio suitable for FTS. Fig. 8(a) shows the effect of temperature and H_2/CO_2 molar ratio in the feed over the H_2/CO molar ratio obtained in the product gases. It can be seen that for a constant H_2/CO_2 ratio, higher temperature (900 °C), causes a drop in H_2/CO molar ratio as compared to lower temperature (750 °C). For a H_2/CO_2 molar ratio of 1.3, H_2/CO molar ratio at 750 °C and 900 °C is 1.94 and 1.75 respectively. On the

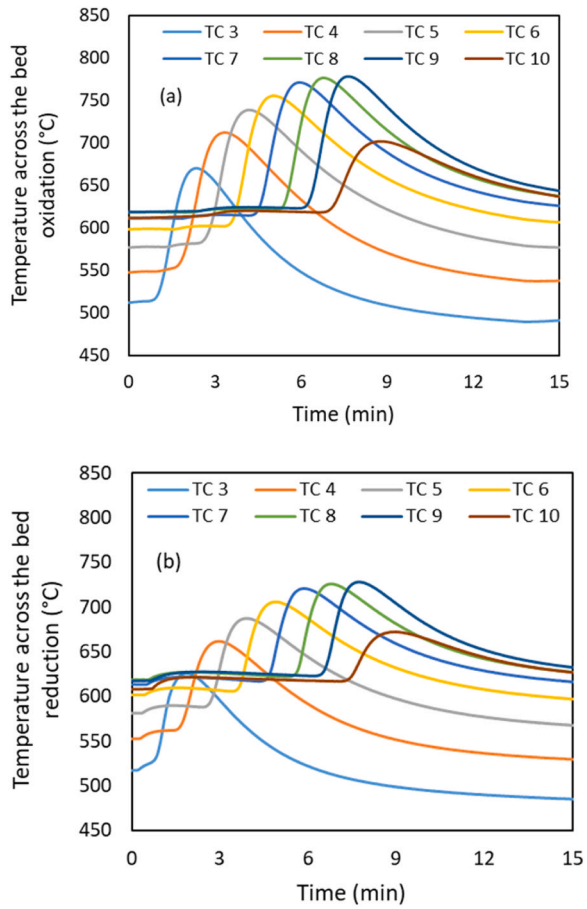

Fig. 6. (a) Evolution of temperature profile during the Cu oxidation with 10% O_2 feed and (right) CuO reduction with 20% H_2 feed gas at 600 °C, 1.0 bar and a feed composition of 10% vol. O_2 in N_2.

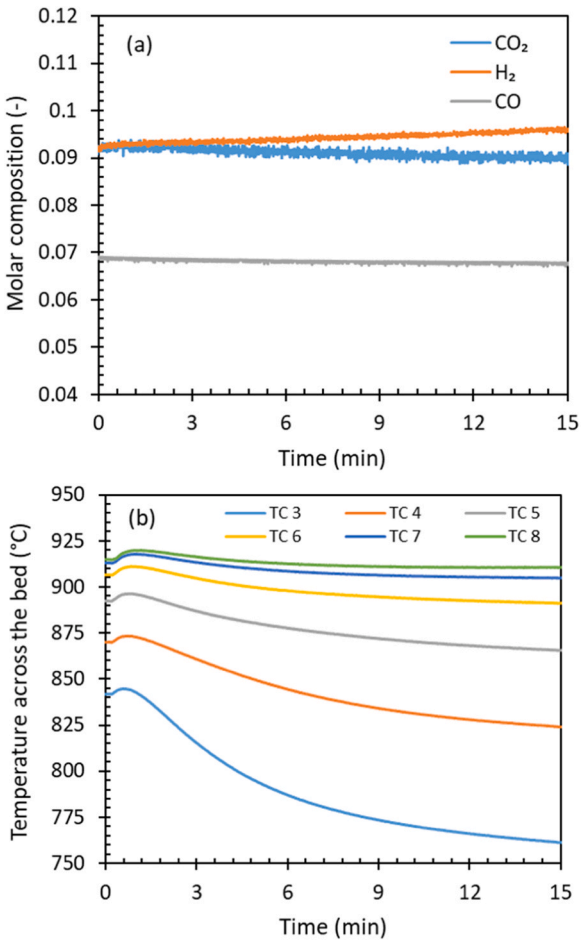

Fig. 7. a) The product gas molar composition and b) temperature profiles during the RWGS stage at 900 °C, 1.0 bar H_2/CO_2 equal to 1.

other hand, higher H_2/CO_2 molar ratio causes H_2/CO molar ratio higher than 2.0 in the product gases.

To further explore the effect of temperature on H_2/CO molar ratio, a wide range of temperatures (650 – 900 °C) is studied in Fig. 9 and results are compared with the equilibrium values obtained through Gibbs reactor simulation using Aspen PLUS® software (and neglecting the formation of CH_4). It can be seen that H_2/CO molar ratio during the experiments is always higher than the equilibrium values, showing that the feed conversion during the experiments is always less than the equilibrium values. But, as the temperature is increased from 650 °C to 900 °C, the experimental results move closer to the equilibrium values but at the expense of lower H_2/CO ratio in the product. The results show that a H_2/CO_2 molar ratio in the range of 1.0 – 1.3 and an operating temperature of 700 – 800 °C is favourable for a H_2/CO molar ratio close to 2.0. Additionally, by increasing the temperature CO_2/CO ratio increases (Fig. 8(b)) confirming the behaviour of the material to operate close to chemical equilibrium conditions and therefore with high fidelity in the performance and control of the syngas composition at different operating conditions.

In Fig. 10 (a), the effect of pressure (1 – 8 bar) over H_2/CO molar ratio in the product has been studied. It can be seen that higher pressure slightly favours the H_2/CO molar ratio in the product but H_2/CO molar ratio decreases as temperature increases from 650 to 900 °C. In Fig. 10 (c and d), the impact of temperature on CO_2 and H_2 conversion within the product during the RWGS process, maintaining a H_2/CO_2 molar ratio of 1.3 in the feed has been observed. The experimental findings have been compared against equilibrium predictions. Notably, the peak CO_2 and H_2 conversion, reaching 60% and 45% respectively at equilibrium, occurs at 900 °C. However, during experimentation under identical operating conditions, the achieved CO_2 and H_2 conversion rate is slightly lower, at 50% and 30% respectively. The unconverted CO_2 could be recovered before or after the FTS and re-used in the RWGS thus reducing the CO_2 import, or it can act as a dry reforming agent for the light hydrocarbons (C_1-C_4) which generates in the FTS reactor. Nonetheless, both the equilibrium and experimental results exhibit a similar overall trend.

Finally, the CO_2-to-CO conversion is plotted in Fig. 11 as measured at different conditions. The materials could achieve up to 50% of CO_2-to-CO conversion at 850 and 900°C and 1.3 H_2/CO_2 molar ratio and resulting H_2/CO of 1.9. this number is approximately 80% of the expected conversion at thermodynamic equilibrium. Therefore, this result represents the expected performance of the system which should be used to assess the quality fo the process overall and used as terms of comparison with respect to other processes.

3.3. Complete cycle of CL-RWGS

A complete cycle of CL-RWGS using Cu-based OC has been performed at pseudo-adiabatic conditions. Repeated cycles of the material under real CL-RWGS conditions are assessed for the first time under continuous operation. This demonstrated the validity of the concept in terms of gas production (H_2/CO ratio, CO_2 conversion) and thermal management. The conditions used for the Cu-oxidation, CuO reduction, RWGS and purge stages have been tabulated in Table 3. The pseudo-adiabatic conditions were achieved by fixing the furnace temperature to minimum values (500 °C, 550 °C and 600 °C) to avoid the reactor

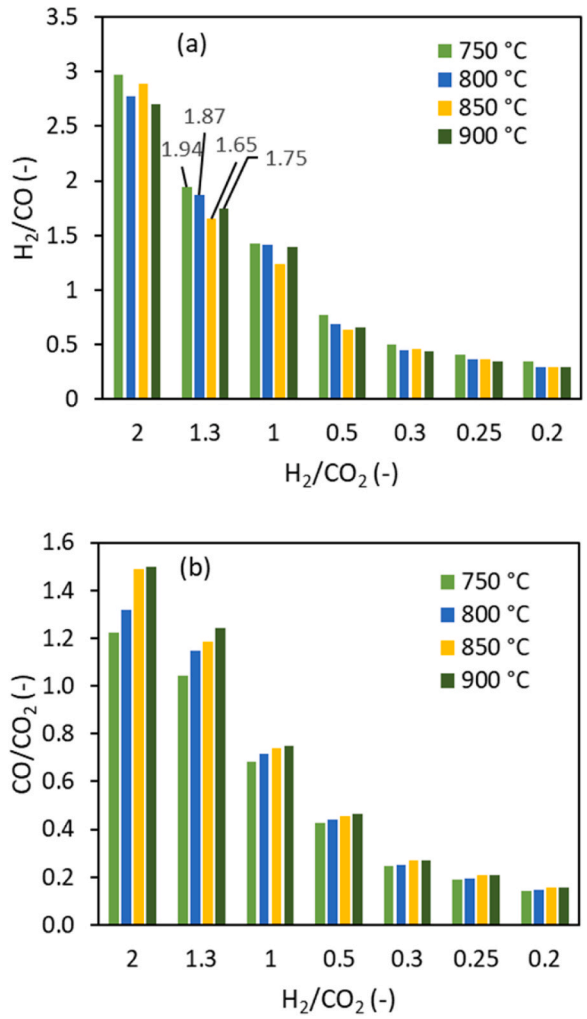

Fig. 8. The effect of feed composition (H_2/CO_2 molar ratio) and temperature on the a) H_2/CO and b) CO/CO_2 molar ratio in the product gases during the RWGS process.

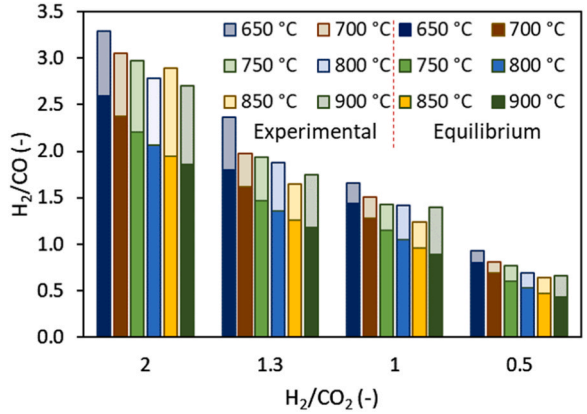

Fig. 9. The effect of feed composition (H_2/CO_2 molar ratio) and temperature on the H_2/CO molar ratio in the product during the RWGS process. Experimental results are compared with the equilibrium findings.

solid temperature going lower than that value. Lab-scale reactors are dominated by heat losses, therefore, a thermal input is required to limit the cooling of the system. On the other hand, industrial-scale (adiabatic) reactor presents limited heat losses (to avoid loss of efficiencies) given their large diameter therefore the minimum temperature of the reactor is dictated by process feeding conditions and the interaction between reactions and heat axial and radial fronts. In this experimental campaign, the furnace temperature set point indicated the minimum temperature of gas reactants. Therefore any additional heat generated in the bed (by Cu-CuO redox reactions) is then removed by catalytic RWGS and the inevitable heat losses that are generated when the solid temperature is > the furnace setpoint.

Despite the RWGS is barely affected by pressure on the H_2/CO ratio, to provide a full understanding of the process, continuous multiple cycles have been carried out at 1 bar and 5 bar. This comparison is relevant from fundamental and design perspectives because: i) syngas generation is likely to operate at high pressure therefore to reduce costs of compression given the conventional operating conditions of liquid fuel synthesis of chemical transformation; ii) chemical looping at atmospheric pressure has been widely discussed and presented with fluidised bed reactors but continuous operation at high pressure has never been achieved unless packed bed reactors of gas switching reactors [32, 37–39]; iii) at constant gas flowrates, increasing the operating pressure reduces the superficial gas velocity and the residence time and has some negative impact on Cu kinetics [40–43].

Fig. 12 (a – b) shows the single stage molar composition and temperature profile across the reactor at 600 °C, 1 bar and H_2/CO_2 molar ratio of 1.0. During the oxidation stage, diluted air (10% O_2 in feed) was fed in the reactor at 600 °C and 1 bar for 324 s with the main product being N_2 and He as can be seen in Fig. 12 (a). This oxidation caused a rise of max 184 °C in the bed. The supply of air was turned off at 324 s before the O_2 breakthrough. After the oxidation, the reactor was purged for 140 s using 4 NLPM of pure N_2 to remove the O_2 from the reactor before starting the next reaction stage. During the reduction and RWGS stages, a gas mixture of H_2/CO_2 was fed in the reactor for 320 s. In the initial phase of this reaction stage, H_2 in the feed reduced the CuO therefore only CO_2 is detected at the outlet (on a dry gas). After 162 s of this stage, once the reduction is finished, H_2 and CO_2 reacts through the RWGS reaction (R3) and produce syngas (H_2/CO molar ratio = 2.0). The results show that a H_2/CO molar ratio of 2.0 has been achieved in this case. Once a steady state composition of syngas is obtained, 8 NLPM of pure N_2 were fed for 140 s to remove the syngas from the reactor before the start of second oxidation stage.

The experiment has been designed to retain a significant amount of heat during the initial stages of the RWGS process, as shown in Fig. 12 (b). The maximum temperature within the bed is observed at the conclusion of the reduction phase, specifically at a bed length of 135 mm, corresponding to 785 °C. This condition leads to enhanced feed conversion and a reduced release of H_2 in the resulting product gases. It must be noted that the end of oxidation and the end of the reduction almost overlaps while, under adiabatic (or limited heat losses) the bed would have further increased its solid temperature. Instead, during purge, the bed already exhibits a partial cooling. Throughout the process of RWGS, a substantial portion of the heat is extracted, leaving only the final segment of the bed at 673 °C. This particular section of the bed corresponds to the point where the molar ratio of H_2/CO in the product attains a value of 2.0.

In order to assess the stability of the material and ensure the replicability of experimental outcomes, a comprehensive investigation involving the execution of five complete cycles of CL-RWGS was conducted. The experimentation was carried out under controlled operational parameters, specifically at a temperature of 600 °C, 1 bar, and a H_2/CO_2 molar ratio of at 1.0, as depicted in Fig. 13. The consistent and repeatable outcomes show the validity of the process under relevant conditions and the material's suitability to operate as an OC and a catalyst within the context of the CL-RWGS process.

To investigate the sensitivity of the CL-RWGS process across a range of temperatures (500 – 600 °C), pressures (1 – 5 bar), and H_2/CO_2 molar ratios (1.0 – 1.3), experimental studies were carried out, and the resulting graphical representations are presented in the Supplementary

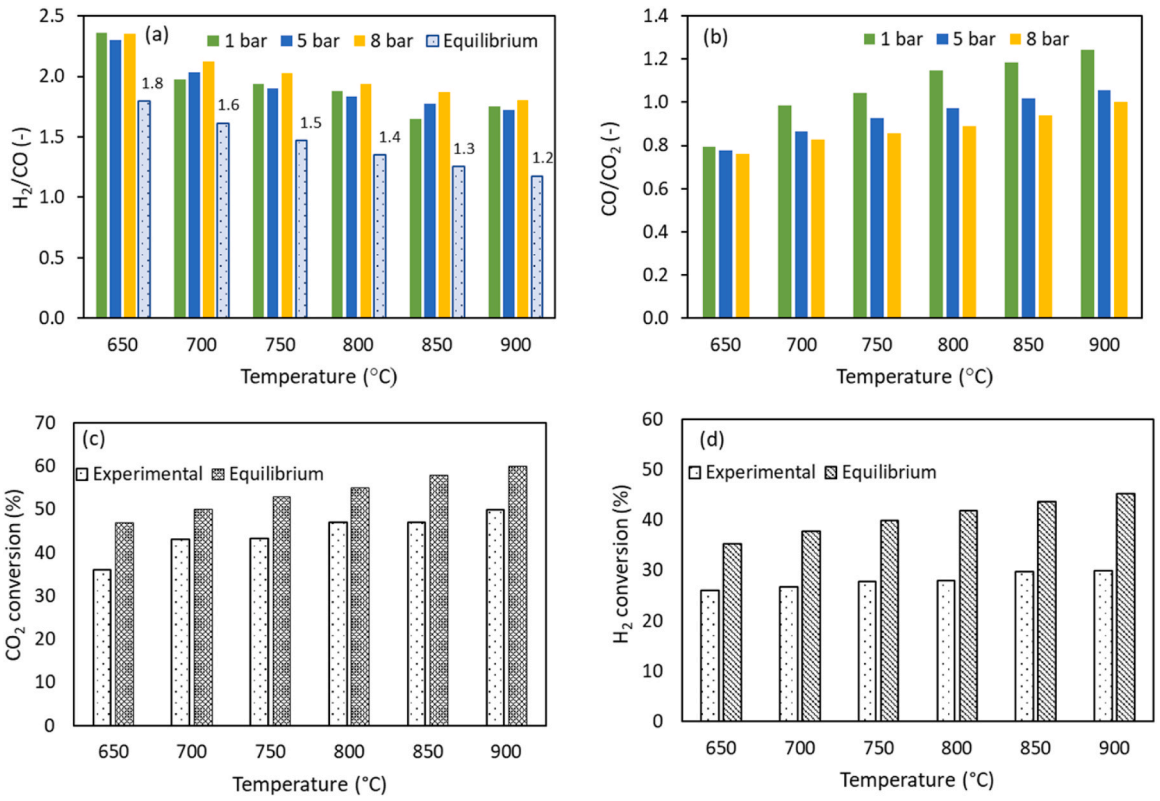

Fig. 10. Effect of temperature and pressure on the a) H_2/CO, b) CO/CO_2 molar ratio in the product, c) CO_2 conversion and d) H_2 conversion during the RWGS process at H_2/CO_2 molar ratio of 1.3 in the feed. Experimental results are compared with the equilibrium findings.

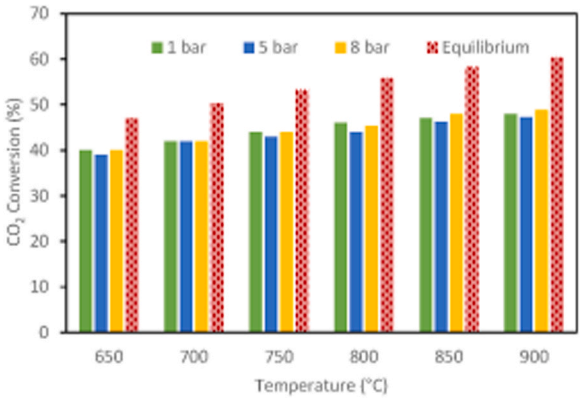

Fig. 11. Effect of temperature and pressure on the CO_2-to-CO conversion during the RWGS process at H_2/CO_2 molar ratio of 1.3 in the feed.

Table 3
The inlet conditions for the complete cycle of CL-RWGS (furnace temperature at 500 – 600 °C and pressure at 1 – 5 bar).

Conditions	Oxidation	Purge – I	Reduction + RWGS	Purge – II
Flow rate [NLPM]	10	4	16	8
Feed time [s]	324	140	320	140
Mole fraction [%]				
N_2	79.5	100	47 – 50	100
O_2	10.5	_	_	_
He	10	_	6	_
H_2	_	_	24 – 25	_
CO_2	_	_	19 – 24	_

Data. A concise summary of these sensitivity analyses is provided in Table 4. The consecutive cycles of CL-RWGS under various temperature and pressure conditions demonstrated that this system is suitable for further scale up and can be implemented at industrial scale.

As the temperature falls below 600 °C at 1 bar pressure and a H_2/CO_2 molar ratio of 1.3, there is a significant increase in the resulting H_2/CO molar ratio which exceeds the optimal value of 2.0 for FTS. This higher ratio at lower temperatures, specifically 3.14 at 500 °C, is not ideal. This decrease in H_2/CO molar ratio is mainly due to a rise in ΔT for both the oxidation and reduction stages. This leads to more conversion of H_2 during the RWGS stage, resulting in a lower H_2/CO molar ratio at higher temperatures. Furthermore, as the H_2/CO_2 molar ratio in the feed is reduced from 1.3 to 1.0, under the 600 °C and 1 bar operating conditions, the resulting H_2/CO molar ratio decreases from 2.35 to the desired value of 2.0 for FTS. This shows a direct connection between the composition of the feed and the resulting gas product, emphasizing the importance of carefully controlling operational parameters for optimizing the product composition and at the same time the flexibility in tailoring the process for different uses.

While the breakthrough times for oxidation and reduction stages remain quite similar across temperatures (500 – 600 °C) at 1 bar pressure, at higher pressures (5 bar) the breakthrough time increases in both oxidation and reduction. This can be explained by a lower superficial gas velocity and increased residence time that facilitates the O_2 and H_2 to reach more Cu/CuO sites in the particle. While the effect on RWGS is marginal, higher pressure is relevant to increase the cycle time and Cu utilisation during the redox cycles. Finally, as anticipated in the previous section, the multiple cycle tests can achieve up to 48% CO_2-to-CO conversion for a 200 s, approximately 90% of the total time on stream during the RWGS stage considering that the RWGS occurs under dynamic operation with a temperature change along the bed from 750°C (end of the reduction) to 650°C (end of the RWGS) as reported in Fig. 12 (b) for the entire period of the RWGS stage. To the author's knowledge,

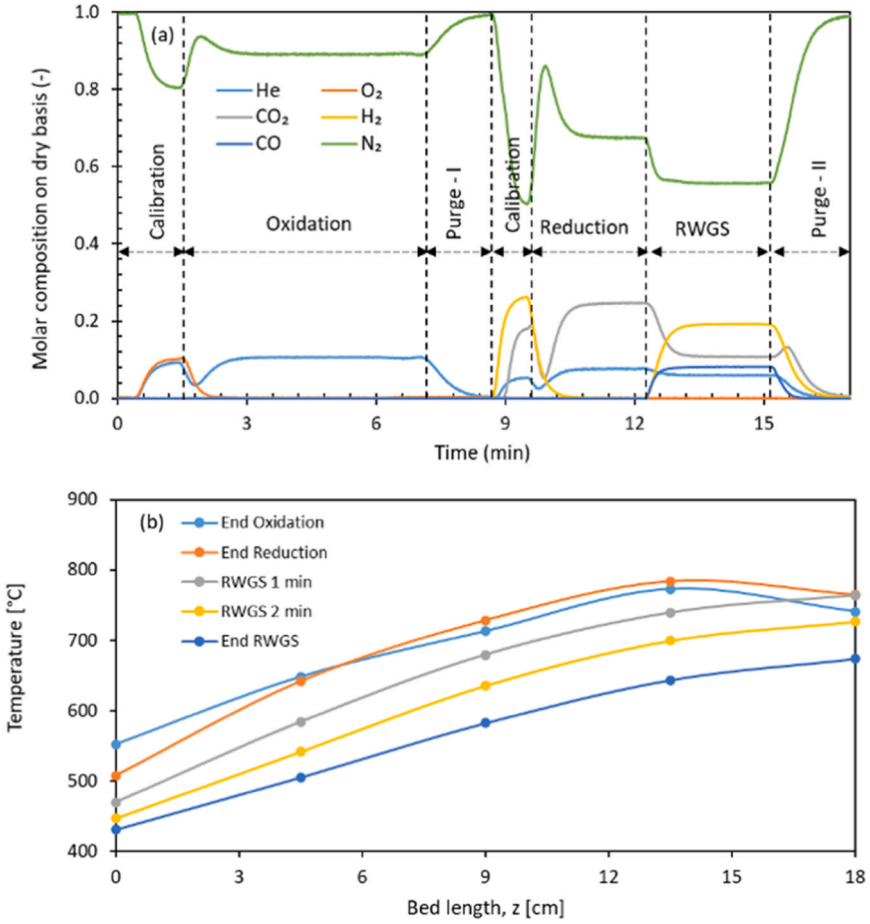

Fig. 12. a) Molar composition and b) axial temperature profile during one complete cycle of CL-RWGS process at 600 °C, 1 bar and H_2/CO_2 molar ratio of 1.0 in the feed.

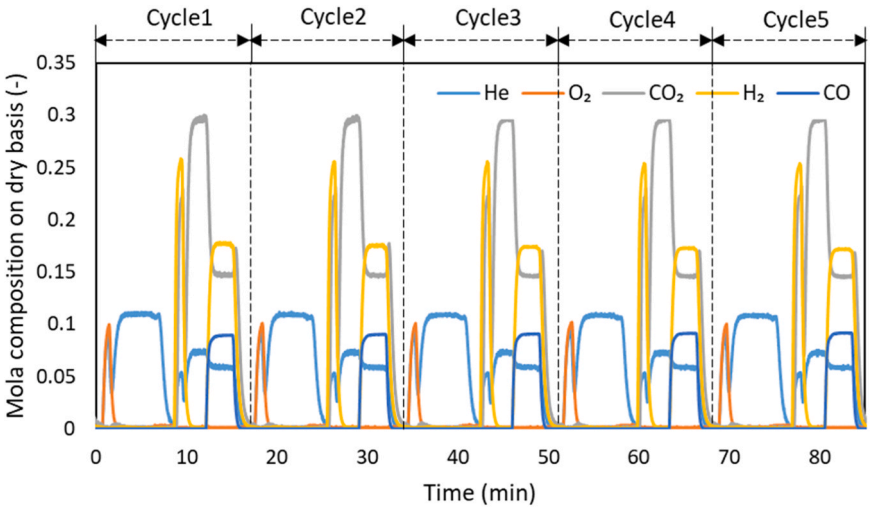

Fig. 13. Molar composition profile during five complete cycles of CL-RWGS process at 600 °C, 1 bar and H_2/CO_2 molar ratio of 1.0 in the feed.

better CO_2-to-CO conversion are reported in literature using direct reduction of CO_2 (e.g. Bulfin et al. [24] claimed a 80% CO_2 conversion), however, those results are limited to a peak conversion and very dispersive results using 80 g of CeO_2 reactor size and feeding gas of 0.3 SLPM with 5% of CO_2 which is approximately 200 times lower than the case presented here. Finally, the 200–300 seconds RWGS cycle allowed for continuous syngas production before transitioning to CL-RWGS, crucial for maintaining oxygen carrier capacity and avoiding temperature decrease due to the endothermic RWGS process.

CL-RWGS offers significant engineering advantages over externally-heated RWGS systems. While externally-heated RWGS requires low-carbon fuels (e.g. H_2) or additional post-combustion capture for carbon-neutral product generation, CL-RWGS facilitates the production of pure or concentrated CO_2, which is readily recoverable at a low cost.

Table 4
Summary of main performance results during the CL-RWGS process.

Feed Conditions			H_2/CO	CO_2-to-CO conversion [%]	Maximum ΔT achieved [°C]		BT time [s]		Time of continuous syngas generation [s]
Temperature [°C]	Pressure [bar]	H_2/CO_2			$\Delta T_{max, oxi}$	$\Delta T_{max, red}$	Oxi	Red	
500	1	1.3	3.14	41	168	106	330	168	300
550	1	1.3	2.99	43.6	171	118	324	163	200
600	1	1.3	2.35	48.2	184	132	324	163	200
600	1	1.0	2.00	46	184	123	324	163	200
600	5	1.0	2.00	46	184	123	500	204	200

Moreover, CL-RWGS operates within a refractory-lined high-pressure vessel, significantly reducing fabrication expenses compared to the exposed RWGS tubes in externally-heated systems. This process also shows flexibility in accommodating low-quality feedstocks during the reduction stage and enables modular plant design, as plant size is not limited by performance or engineering constraints. By optimizing material formulation, higher CO_2 conversion rates can be achieved. Despite the tested material's design not being specific to this process, CO_2 conversion can reach up to 60% at equilibrium for the H_2/CO_2 molar ratio studied. Additionally, there is potential for exploring novel configurations where CL-RWGS is aided by CO_2-to-CO thermochemical reduction, a chemical looping process, presenting the opportunity for even higher CO_2 conversion rates, although this technology is still in the developmental phase.

4. Conclusion

In this work, the CL-RWGS process using Cu-based OC has been studied under various relevant conditions of temperature and pressure. The analysis carried out on individual reaction stage have confirmed the high performance of Cu/CuO pair a stable and highly selective oxygen carrier in chemical looping. At the same, the reduced Cu as a catalyst for RWGS exhibited up to 48% of CO_2-to-CO conversion and high flexibility to tailor the syngas composition by changing feed gas composition and reaction operating temperature. For the case FTS application, an H_2/CO_2 feed composition between 1.0 and 1.3 is suitable to obtain a H_2/CO ratio close to 2.0. The multiple cycles of CL-RWGS gave stable and reproducible results in terms of H_2/CO molar ratio in the product. Despite being a lab-scale reactor, the process at pseudo-adiabatic conditions demonstrated that continuous CO_2-to-CO conversion of 48% is acheivable when operating the reactor with a minimum temperature of 600 °C, 1 bar and H_2/CO_2 molar ratio 1.0. CL-RWGS provides engineering advantages, enabling cost-effective CO_2 production in a high-pressure vessel and enhancing flexibility with low-quality feedstocks. Despite the unoptimized material, CO_2 conversion rates can reach 60% at equilibrium, with potential for further improvement through future advancements. While further studies are required to understand the optimal conditions, further developments will include the scale-up the technology, expected economics, and overall process assessment under different scenarios.

CRediT authorship contribution statement

Alvaro Amieiro: Writing – review & editing, Supervision, Resources. **Christopher de Leeuwe:** Writing – review & editing, Investigation, Formal analysis. **Vincenzo Spallina:** Writing – review & editing, Supervision, Project administration, Funding acquisition, Conceptualization. **Stephen Poulston:** Writing – review & editing, Resources, Conceptualization. **Syed Zaheer Abbas:** Writing – original draft, Methodology, Investigation, Formal analysis, Data curation, Conceptualization.

Declaration of Competing Interest

The authors declare that they have no known competing financial interests or personal relationships that could have appeared to influence the work reported in this paper.

Data Availability

Data will be made available on request.

Acknowledgements

The authors acknowledge the financial support from the EPSRC BREINSTORM project, EP/S030654/1. The work has also received funding from the European Union's Horizon 2020 research and innovation programme under grant agreement no. 884418 (C4U project). The work reflects only the authors' views and the European Union is not liable for any use that may be made of the information contained therein.

Appendix A. Supporting information

Supplementary data associated with this article can be found in the online version at doi:10.1016/j.jcou.2024.102775.

References

[1] U. IEA, Technology roadmap: carbon capture and storage in industrial applications, International Energy Agency, United Nations Industrial Development Organizations, 2011.
[2] World Steel Organisation .
[3] M. Bui, et al., Carbon capture and storage (CCS): the way forward, in: Energy and Environmental Science, vol. 11, Royal Society of Chemistry, 2018, pp. 1062–1176, https://doi.org/10.1039/c7ee02342a.
[4] Y.A. Daza, J.N. Kuhn, CO 2 conversion by reverse water gas shift catalysis: comparison of catalysts, mechanisms and their consequences for CO 2 conversion to liquid fuels, RSC Adv. vol. 6 (55) (2016) 49675–49691.
[5] Y.A. Daza, J.N. Kuhn, CO 2 conversion by reverse water gas shift catalysis: comparison of catalysts, mechanisms and their consequences for CO 2 conversion to liquid fuels, RSC Adv. vol. 6 (55) (2016) 49675–49691.
[6] P. Kaiser, R.B. Unde, C. Kern, A. Jess, Production of liquid hydrocarbons with CO2 as carbon source based on reverse water-gas shift and fischer-tropsch synthesis, Chem. Ing. Tech. vol. 85 (4) (2013) 489–499, https://doi.org/10.1002/cite.201200179.
[7] Johnson Matthey, JM launches HyCOgen, an enabling technology to efficiently convert CO2 and green hydrogen into sustainable aviation fuel. [Online]. Available: ⟨https://matthey.com/news/2022/hycogen⟩.
[8] Topsoe, "eREACT™ Fuels: New technology essential for electrofuels production. [Online]. Available: ⟨https://www.topsoe.com/our-resources/knowledge/our-products/equipment/e-react-fuels#:~:text=Byutilizing electrical heating in stead,rating that can exceed 95%25⟩.
[9] S. Dzuryk, E. Rezaei, Intensification of the reverse water gas shift reaction by water-permeable packed-bed membrane reactors, Ind. Eng. Chem. Res. vol. 59 (42) (2020) 18907–18920, https://doi.org/10.1021/acs.iecr.0c02213.
[10] S. Thor Wismann, K. Larsen, P. Mølgaard Mortensen, Electrical reverse shift: sustainable CO 2 valorization for industrial scale, Angew. Chem. vol. 134 (8) (2022) 2–5, https://doi.org/10.1002/ange.202109696.
[11] L. Liu, J. Dai, Z. Yang, Y. Li, X. Su, Z. Zhang, Plasma-catalytic carbon dioxide conversion by reverse water–gas shift over La0.9Ce0.1B0.5B'0.5O3-δ perovskite-derived bimetallic catalysts, Chem. Eng. J. vol. 431 (P1) (2022) 134009, https://doi.org/10.1016/j.cej.2021.134009.

[12] L.E. Basini, F. Furesi, M. Baumgärtl, N. Mondelli, G. Pauletto, CO2 capture and utilization (CCU) by integrating water electrolysis, electrified reverse water gas shift (E-RWGS) and methanol synthesis, J. Clean. Prod. vol. 377 (2022), https://doi.org/10.1016/j.jclepro.2022.134280.
[13] E. Delikonstantis, et al., Valorizing the steel industry off-gases: proof of concept and plantwide design of an electrified and catalyst-free reverse water – gas-shift-based route to methanol, Environ. Sci. Technol. (2023), https://doi.org/10.1021/acs.est.3c05246.
[14] M. González-Castaño, B. Dorneanu, H. Arellano-García, The reverse water gas shift reaction: A process systems engineering perspective, React. Chem. Eng. vol. 6 (6) (2021) 954–976, https://doi.org/10.1039/d0re00478b.
[15] R. Iwama, K. Takizawa, K. Shinmei, E. Baba, N. Yagihashi, H. Kaneko, Design and analysis of metal oxides for CO2 Reduction using machine learning, transfer learning, and Bayesian Optimization, ACS Omega vol. 7 (12) (2022) 10709–10717, https://doi.org/10.1021/acsomega.2c00461.
[16] M. Wenzel, et al., CO production from CO2 via reverse water–gas shift reaction performed in a chemical looping mode: Kinetics on modified iron oxide, J. CO2 Util. vol. 17 (2017) 60–68.
[17] V. Singh, L.C. Buelens, H. Poelman, M. Saeys, G.B. Marin, V.V. Galvita, Carbon monoxide production using a steel mill gas in a combined chemical looping process, J. Energy Chem. vol. 68 (2022) 811–825, https://doi.org/10.1016/j.jechem.2021.12.042.
[18] J.I. Makiura, S. Kakihara, T. Higo, N. Ito, Y. Hirano, Y. Sekine, Efficient CO2 conversion to CO using chemical looping over Co-In oxide, Chem. Commun. vol. 58 (31) (2022) 4837–4840, https://doi.org/10.1039/d2cc00208f.
[19] Y.A. Daza, D. Maiti, R.A. Kent, V.R. Bhethanabotla, J.N. Kuhn, Isothermal reverse water gas shift chemical looping on La0.75Sr0.25Co(1-Y)FeYO3 perovskite-type oxides, Catal. Today vol. 258 (2015) 691–698, https://doi.org/10.1016/j.cattod.2014.12.037.
[20] Y.A. Daza, R.A. Kent, M.M. Yung, J.N. Kuhn, Carbon dioxide conversion by reverse water-gas shift chemical looping on perovskite-type oxides, Ind. Eng. Chem. Res. vol. 53 (14) (2014) 5828–5837, https://doi.org/10.1021/ie5002185.
[21] B.J. Hare, D. Maiti, Y.A. Daza, V.R. Bhethanabotla, J.N. Kuhn, Enhanced CO2 conversion to CO by silica-supported perovskite oxides at low temperatures, ACS Catal. vol. 8 (4) (2018) 3021–3029, https://doi.org/10.1021/acscatal.7b03941.
[22] C. de Leeuwe, et al., Thermochemical syngas generation via solid looping process: An experimental demonstration using Fe-based material, Chem. Eng. J. vol. 453 (2023), https://doi.org/10.1016/j.cej.2022.139791.
[23] F. Orsini, et al., Exsolution-enhanced reverse water-gas shift chemical looping activity of Sr2FeMo0.6Ni0.4O6-δ double perovskite, Chem. Eng. J. vol. 475 (2023) 146083, https://doi.org/10.1016/j.cej.2023.146083.
[24] B. Bulfin, M. Zuber, O. Gräub, A. Steinfeld, Intensification of the reverse water–gas shift process using a countercurrent chemical looping regenerative reactor, Chem. Eng. J. vol. 461 (2023) 141896, https://doi.org/10.1016/j.cej.2023.141896.
[25] S.Z. Abbas, J.R. Fernández, A. Amieiro, M. Rastogi, J. Brandt, V. Spallina, Lab-scale experimental demonstration of Ca[sbnd]Cu chemical looping for hydrogen production and in-situ CO<inf>2</inf> capture from a steel-mill, Fuel Process. Technol. vol. 237 (2022), https://doi.org/10.1016/j.fuproc.2022.107475.
[26] C. de Leeuwe, S.Z. Abbas, A. Amieiro, S. Poulston, V. Spallina, Carbon-neutral and carbon-negative chemical looping processes using glycerol and methane as feedstock, Fuel vol. 353 (2023) 129001, https://doi.org/10.1016/j.fuel.2023.129001.
[27] M. Zhu, Q. Ge, X. Zhu, Catalytic reduction of CO 2 to CO via reverse water gas shift reaction: recent advances in the design of active and selective supported metal catalysts, Trans. Tianjin Univ. vol. 26 (3) (2020) 172–187.
[28] D.U. Nielsen, X.M. Hu, K. Daasbjerg, T. Skrydstrup, Erratum to: Chemically and electrochemically catalysed conversion of CO2 to CO with follow-up utilization to value-added chemicals (Nature Catalysis, (2018), 1, 4, (244-254), 10.1038/s41929-018-0051-3), in: Nature Catalysis, vol. 2, Nature Publishing Group, 2019, p. 95, https://doi.org/10.1038/s41929-018-0152-z.
[29] S. Saeidi, et al., Mechanisms and kinetics of CO2 hydrogenation to value-added products: A detailed review on current status and future trends, Renew. Sustain. Energy Rev. vol. 80 (2017) 1292–1311.
[30] F. Vidal Vázquez, P. Pfeifer, J. Lehtonen, P. Piermartini, P. Simell, V. Alopaeus, Catalyst screening and kinetic modeling for CO production by high pressure and temperature reverse water gas shift for fischer-tropsch applications, Ind. Eng. Chem. Res. vol. 56 (45) (2017) 13262–13272, https://doi.org/10.1021/acs.iecr.7b01606.
[31] P. Kaiser, R.B. Unde, C. Kern, A. Jess, Production of liquid hydrocarbons with CO2 as carbon source based on reverse water-gas shift and fischer-tropsch synthesis, Chem. -Ing. -Tech. vol. 85 (4) (2013) 489–499, https://doi.org/10.1002/cite.201200179.
[32] P. Alexandros Argyris, et al., Chemical looping reforming for syngas generation at real process conditions in packed bed reactors: an experimental demonstration, Chem. Eng. J. vol. 435 (2022), https://doi.org/10.1016/j.cej.2022.134883.
[33] S.Z. Abbas, J.R. Fernández, A. Amieiro, M. Rastogi, J. Brandt, V. Spallina, Lab-scale experimental demonstration of Ca[sbnd]Cu chemical looping for hydrogen production and in-situ CO2 capture from a steel-mill, Fuel Process. Technol. vol. 237 (2022), https://doi.org/10.1016/j.fuproc.2022.107475.
[34] G. Grasa, M. Díaz, J.R. Fernández, A. Amieiro, J. Brandt, J.C. Abanades, Blast furnace gas decarbonisation through calcium assisted steel-mill off-gas Hydrogen production. Experimental and modelling approach, Chem. Eng. Res. Des. vol. 191 (2023), https://doi.org/10.1016/j.cherd.2023.01.047.
[35] G. Grasa, M. Díaz, J.R. Fernández, A. Amieiro, J. Brandt, J.C. Abanades, Blast furnace gas decarbonisation through Calcium Assisted Steel-mill Off-gas Hydrogen production. Experimental and modelling approach, Chem. Eng. Res. Des. vol. 191 (2023) 507–522, https://doi.org/10.1016/j.cherd.2023.01.047.
[36] M. Díaz, M. Alonso, G. Grasa, J.R. Fernández, The Ca-Cu looping process using natural CO2 sorbents in a packed bed: Operation strategies to accommodate activity decay, Chem. Eng. Sci. vol. 273 (2023) 118659, https://doi.org/10.1016/j.ces.2023.118659.
[37] H.P. Hamers, F. Gallucci, P.D. Cobden, E. Kimball, M. van Sint Annaland, CLC in packed beds using syngas and CuO/Al2O3: Model description and experimental validation, Appl. Energy vol. 119 (Apr. 2014) 163–172, https://doi.org/10.1016/j.apenergy.2013.12.053.
[38] F. Gallucci, H.P.P. Hamers, M. van Zanten, M. van Sint Annaland, Experimental demonstration of chemical-looping combustion of syngas in packed bed reactors with ilmenite, Chem. Eng. J. vol. 274 (Apr. 2015) 156–168, https://doi.org/10.1016/j.cej.2015.03.081.
[39] M. Osman, M.N. Khan, A. Zaabout, S. Cloete, S. Amini, Review of pressurized chemical looping processes for power generation and chemical production with integrated CO2 capture, Fuel Process. Technol. vol. 214 (2021) 106684, https://doi.org/10.1016/j.fuproc.2020.106684.
[40] M.A. San Pio, I. Roghair, F. Gallucci, M. van Sint Annaland, Investigation on the decrease in the reduction rate of oxygen carriers for chemical looping combustion, Powder Technol. vol. 301 (2016) 429–439, https://doi.org/10.1016/j.powtec.2016.06.031.
[41] M.A. San Pio, F. Gallucci, I. Roghair, M. van Sint Annaland, On the mechanism controlling the redox kinetics of Cu-based oxygen carriers, Chem. Eng. Res. Des. (2017), https://doi.org/10.1016/j.cherd.2017.06.019.
[42] R.F. Kooiman, H.P. Hamers, F. Gallucci, M. Van Sint Annaland, Experimental demonstration of two-stage packed bed chemical-looping combustion using syngas with CuO/Al2O3 and NiO/CaAl2O4 as oxygen carriers, Ind. Eng. Chem. Res. vol. 54 (7) (Feb. 2015) 2001–2011, https://doi.org/10.1021/ie5038165.
[43] F. García-Labiano, J. Adánez, L.F. de Diego, P. Gayán, A. Abad, Effect of pressure on the behavior of copper-, iron-, and nickel-based oxygen carriers for chemical-looping combustion, Energy Fuels vol. 20 (1) (2006) 26–33, https://doi.org/10.1021/ef050238e.